New Approach to Intercalibration Using High Spectral Resolution Sounder

TAHARA Yoshihiko*

Abstract

This paper describes how a new intercalibration technique between a broadband sensor and a high spectral resolution sounder (a hyper sounder) is developed. To compare the two sensors, the new technique generates a super channel cloning the broad channel from the hyper sounder by minimizing the spectral response difference. The comparison technique is reviewed by examining that technique to compare brightness temperatures and radiances between the MTSAT-1R imager and the hyper sounder AIRS aboard AQUA. The simulated brightness temperature and radiance of the AIRS super channel for the MTSAT-1R channel IR2 (12 μm) are almost to the same as those of IR2, since AIRS fully covers the IR2 observing band, and the spectral response of the AIRS super channel is nearly the same as that of IR2. Real data comparison is also examined. The residual recognized in the comparison between IR2 and AIRS corresponds well to the comparisons between IR2 and the channel 3B of AVHRR aboard NOAA-18, even though many AIRS channels are missing. The comparisons of the MTSAT-1R channel IR1 (10.8 μm) and IR4 (3.8 μm) with AIRS also show a similarity to the comparisons between MTSAT-1R and AVHRR, even though the AIRS spectral gaps within the IR1 and IR4 bands prevent the generation of the spectral response functions of the AIRS super channels that are exactly the same as those of IR1 and IR4. These results indicate that this intercalibration technique is effective.

1 Introduction

It is important to study the calibration accuracy of space-based sensors, such as the imager aboard MTSAT-1R, after launch. Intercalibration, which is conducted by comparing the observed data of two or more sensors, is one solution. The information obtained from intercalibration is useful in reviewing the hardware and software of the sensor, finding any problems with the sensor, and assisting in the use of observed data. In the past, an intercalibration study between GMS-5 and GOES-9 has been reported (Tahara el al., 2004). The comparison of MTSAT-1R with the imager AVHRR aboard the NOAA satellites is operationally examined, and the results are posted on the Webpage "Monitoring of MTSAT-1R Navigation and Calibration" (MSC).

In the comparison, the observing conditions of the two sensors are expected to be as similar as possible. However, in practice it is difficult to make the conditions exactly the same for both sensors, since there are a lot of factors that can vary such as observing time, observing position, spectral response, footprint shape, and medium of the optical path from observing target to sensor. In general, the differences of time, position, footprint and optical path are the sources of variational errors in the comparison. The variational error can be reduced by specifying strict match-up conditions. However, the spectral response difference between two sensors yields a systematic

* System Engineering Division, Data Processing Department, Meteorological Satellite Center

(Recieved July 27 , 2007, Accepted December 21, 2007)

difference in the result of the comparison, and may hamper using the result in the discussion of sensor calibration. In order to estimate and mitigate the effect of the spectral response difference, radiances simulated by a radiative transfer model may be used. However, this raises another concern about accuracy because of the biases contained in the radiative transfer model and background atmospheric fields.

In 2002, the National Aeronautics and Space Administration (NASA, U.S.) launched a satellite called AQUA. It carries a high spectral resolution sounder (hereinafter called a "hyper sounder") named the Atmospheric Infrared Sounder (AIRS), which observes out-coming radiances from the top of the atmosphere over a wide infrared band using a large number of channels (hereinafter called "hyper channels"), each of which has a narrow bandwidth. In 2006, the European Organization for the Exploitation of Meteorological Satellites (EUMETSAT) also launched a satellite, called METOP-A, which carries a hyper sounder named the Infrared Atmospheric Sounding Interferometer (IASI). Data observed by AIRS and IASI are posted on the Internet. More accurate intercalibration can be expected by using data from the hyper sounder. Gunshor et al. (2006) and Tobin et al. (2006) propose an intercalibration technique that generates a super channel from the hyper channels to evaluate the radiance of an imager channel. This super channel is created by convolving spectral responses between the hyper channels and the broadband channel (the "convolution method").

This report proposes a new technique for use in the intercalibration between the imager channel and the hyper sounder. The technique also generates a super channel from the hyper sounder by adjusting the spectral responses of the two sensors. However, the adjustment is performed by a non-linear optimization computation instead of by the convolution method. Section 2 introduces the methodology of this new intercalibration technique. Section 3 reviews the proposed method by examining MTSAT-1R and AIRS intercalibration. Section 4 discusses the applicability of this method. Finally, section 5 concludes with a summary and an outlook of future work.

2 Super channel of hyper sounder

2.1 Definition of super channel

This section introduces a super channel consisting of a hyper sounder that clones a broadband sensor. In the discussion, the observing conditions are assumed to be the same for the two sensors except for their spectral responses.

Under the same observing conditions, the radiances of the broadband channel and the super channel are expected to be equal. The radiance observed by the broadband channel I_b is the accumulation of the upwelling radiance from the top of the atmosphere $I(\nu)$ with the spectral response function (SRF) of the channel $S_b(\nu)$,

$$I_b = \int S_b(\nu) I(\nu) d\nu, \quad \text{where} \quad \int S_b(\nu) d\nu = 1. \tag{1}$$

ν represents the wavenumber (or wavelength or frequency). Here, $S_b(\nu)$ is normalized as its area so that it equals one. Similarly, the radiance observed by the hyper channel i, whose SRF is $S_i(\nu)$, is written as

$$I_i = \int S_i(\nu) I(\nu) d\nu, \quad \text{where} \quad \int S_i(\nu) d\nu = 1. \tag{2}$$

Assuming that the hyper channels cover the whole band region of the broadband channel, I_b is approximated by the linear combination of $\{I_i\}$,

$$\begin{aligned} I_b &\approx \sum_i w_i I_i \\ &= \sum_i w_i \int S_i(\nu) I(\nu) d\nu \\ &= \int \left\{ \sum_i w_i S_i(\nu) \right\} I(\nu) d\nu. \end{aligned} \tag{3}$$

$\{w_i\}$ represent the weights of the combination. In order to satisfy the approximation (3) for any radiative field $I(\nu)$, the equation,

$$S_b(\nu) \approx \sum_i w_i S_i(\nu), \tag{4}$$

is obtained by comparing (1) and (3). This indicates that the problem of approximating the radiance of the broadband channel from the radiances of the hyper channels is equivalent to the problem of computing a set of the weights $\{w_i\}$ satisfying (4) and generating a super channel whose SRF is

$$S_s(\nu) = \sum_i w_i S_i(\nu). \tag{5}$$

The weights $\{w_i\}$ can be obtained by solving the non-linear optimization problem,

$$\{w_i\} = \mathrm{argmin}\ \ J(w_1, w_2, \cdots), \tag{6}$$

where J is a cost function defined by

$$J(w_1, w_2, \cdots) = \int \left\{ S_b(\nu) - \sum_i w_i S_i(\nu) \right\}^2 d\nu. \tag{7}$$

To solve the problem, the gradient of J may be required.

$$\frac{\partial J}{\partial w_k} = \int 2 S_k \left\{ S_b(\nu) - \sum_{i=1}^{n} w_i S_i(\nu) \right\} d\nu. \tag{8}$$

2.2 Computation of super channel radiance and brightness temperature

The weights $\{w_i\}$ are computed by solving (7). The SRF of the super channel is obtained by substituting $\{w_i\}$ into (5). Since the SRF is an approximation of $S_b(\nu)$, its area is not exactly one. Therefore, the radiance of the super channel I_s is computed by

$$\begin{aligned} I_s &= \frac{\int S_s(\nu) I(\nu) d\nu}{\int S_s(\nu) d\nu} \\ &= \frac{\sum_i w_i \int S_i(\nu) I(\nu) d\nu}{\sum_i w_i \int S_i(\nu) d\nu} \\ &= \frac{\sum_i w_i I_i}{\sum_i w_i}. \end{aligned} \tag{9}$$

The brightness temperature of the super channel T_s is obtained by inverting the equation,

$$I_s = \frac{\int S_s(\nu) B(\nu, T_s) d\nu}{\int S_s(\nu) d\nu}. \tag{10}$$

$B(\nu, T)$ is the monochromatic Planck function computing radiance at the wavenumber ν emitted from the blackbody whose temperature is T. Once $\{w_i\}$ is divided by $\sum_{i=1}^{n} w_i$, the denominator of (9) and (10) can be eliminated.

Since the inversion of (10) requires a lot of computation cost, the sensor Planck function (Weinreb et al., 1981) for the super channel $B_s(T)$

can be used to approximate (10).

$$I_s = B_s(T_s) = \frac{2hc^2(\bar{\nu}_s)^3}{\exp\left(\frac{hc\bar{\nu}_s}{KT_e}\right) - 1}, \quad (11)$$

where

$$T_e \approx c_1 + c_2 T_s. \quad (12)$$

$\bar{\nu}_s$ denotes a wavenumber representing the super channel, T_e is called the effective temperature, and c_1 and c_2 are called band correction coefficients. In general, the approximation of the sensor Planck function is very accurate. The approximation error of (12) is less than 0.01 K.

2.3 Treatment of missing hyper channels

The number of the hyper channels is very large. However, not all observations of the channels are necessarily useful. If there is prior information regarding abnormal channels or low accuracy channels, they can be put on a blacklist and rejected from the super channel. In succeeding, the coefficients of its sensor Planck function should be modified.

$$I'_s = \frac{\sum_{i \notin \text{blacklist}} w'_i I_i}{\sum_{i \notin \text{blacklist}} w'_i}, \qquad T'_s = B'^{-1}_s(I'_s). \quad (13)$$

w'_i represents the weights of the super channel computed by eliminating the blacklisted channels, and B'^{-1}_s represents the inversion of the sensor Planck function for the modified super channel.

If abnormal observations are obtained for some hyper channels outside of the blacklist, it is not practical to regenerate the weights of the super channel and its sensor Planck function every time. It is also not practical to calculate the weights and the sensor Planck functions beforehand for all combinations of missing channels. An easy and practical way is to exclude the missing observations in the radiance computation of the super channel and use the sensor Planck function without modification.

$$I''_s = \frac{\sum_{\substack{i \notin \text{missing} \\ i \notin \text{blacklist}}} w'_i I_i}{\sum_{\substack{i \notin \text{missing} \\ i \notin \text{blacklist}}} w'_i}, \qquad T''_s = B'^{-1}_s(I''_s). \quad (14)$$

The brightness temperature deviation caused by the missing observations is the combination of the radiance deviation $I''_s - I'_s$ and the use of the unsuitable sensor Planck function,

$$T''_s - T'_s = B'^{-1}_s \left(\sum_{\substack{i \notin \text{missing} \\ i \notin \text{blacklist}}} w'_i I_i \Big/ \sum_{\substack{i \notin \text{missing} \\ i \notin \text{blacklist}}} w'_i \right) - T'_s. \quad (15)$$

3 Intercalibration between MTSAT-1R and AIRS

3.1 AIRS super channel for MTSAT

The red lines in Figure 1 show the SRF of the MTSAT-1R channel IR2 (12-micron), and the green lines show the SRFs of AIRS. The SRFs of AIRS are obtained from the Website of the Atmospheric Spectroscopy Laboratory (ASL) in the University of Maryland, Baltimore County (UMBC). More than 300 AIRS channels covering the whole observing band of IR2 are available.

The blue lines in Figure 2 show the SRF of the AIRS super channel for IR2 whose SRF is drawn by the red lines. Even though a small fluctuation is seen in the super channel SRF, it conforms well to the IR2 SRF.

Figure 3 shows the weights of the AIRS channels to

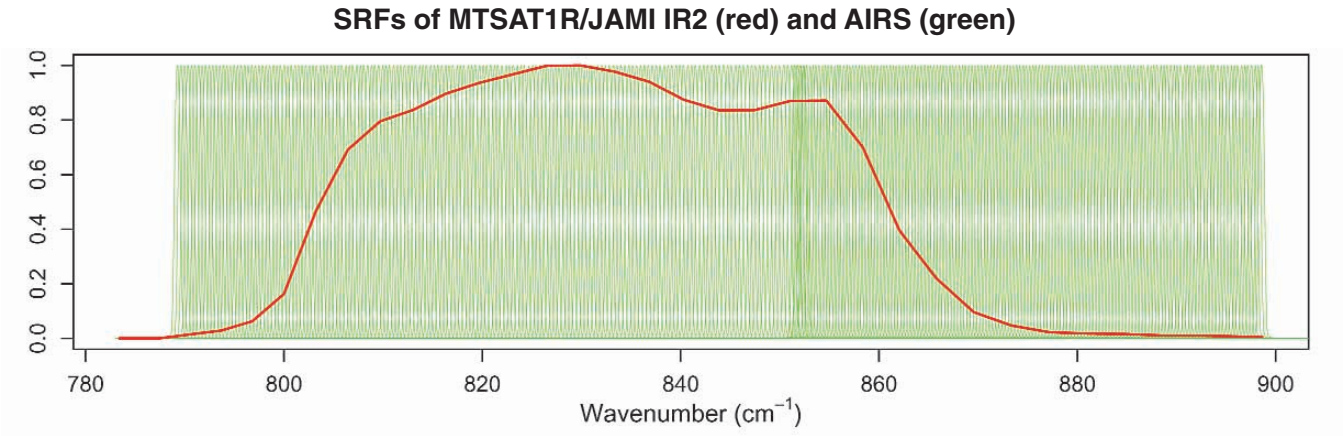

Figure 1: The SRFs of the MTSAT-1R channel IR2 (red) and the AIRS channels (green). There are more than 300 AIRS channels within the IR2 band.

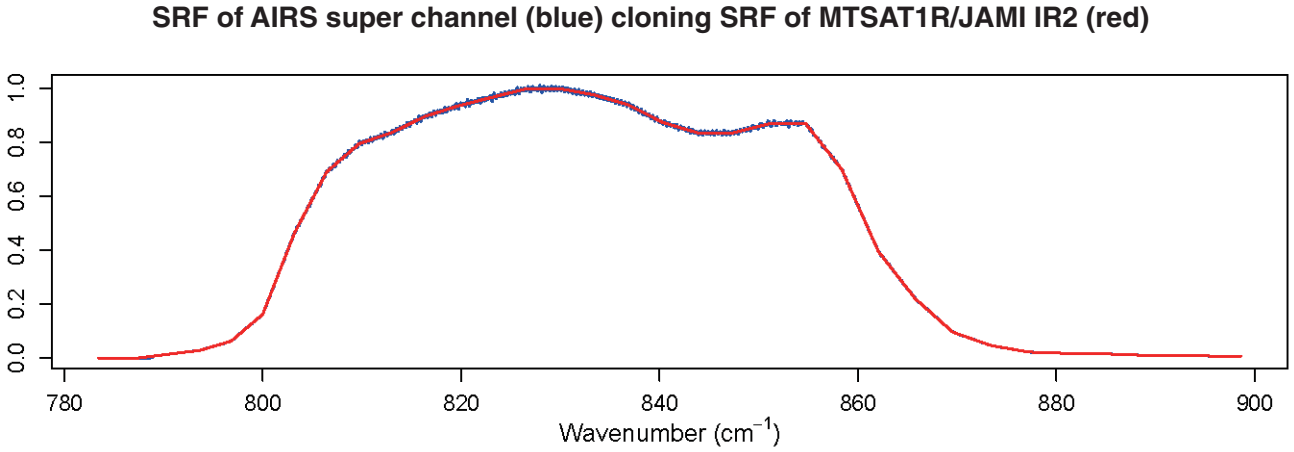

Figure 2: The SRF of the MTSAT-1R channel IR2 (red) and the super channel (blue) consisting of the AIRS channels shown in Figure 1.

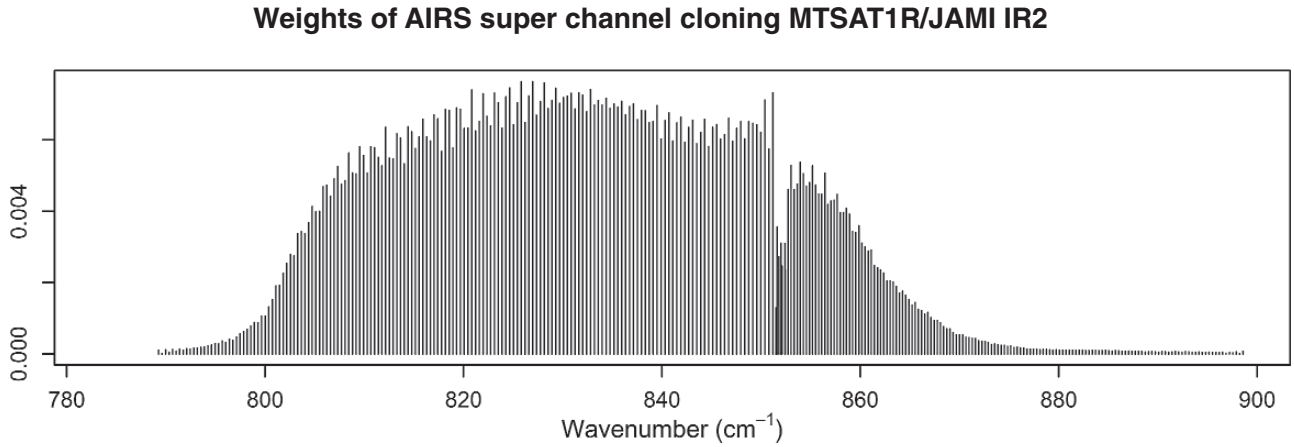

Figure 3: The weights of the AIRS channels constituting the super channel shown in Figure 2.

construct the super channel shown in Figure 2. The weights show similar curves to the IR2 SRF except around 850 cm^{-1} where the AIRS channels overlap each others and the weights of the overlapping channels are relatively smaller than those of the others.

Figure 4 shows the same chart as in Figure 2, but for MTSAT1-R IR1 (10.8-micron), IR3 (6.8-micron) and IR4 (3.8-micron). Since the AIRS channels do not fully cover the observing bands of three MTSAT-1R channels, the SRFs of the super channels contain gaps.

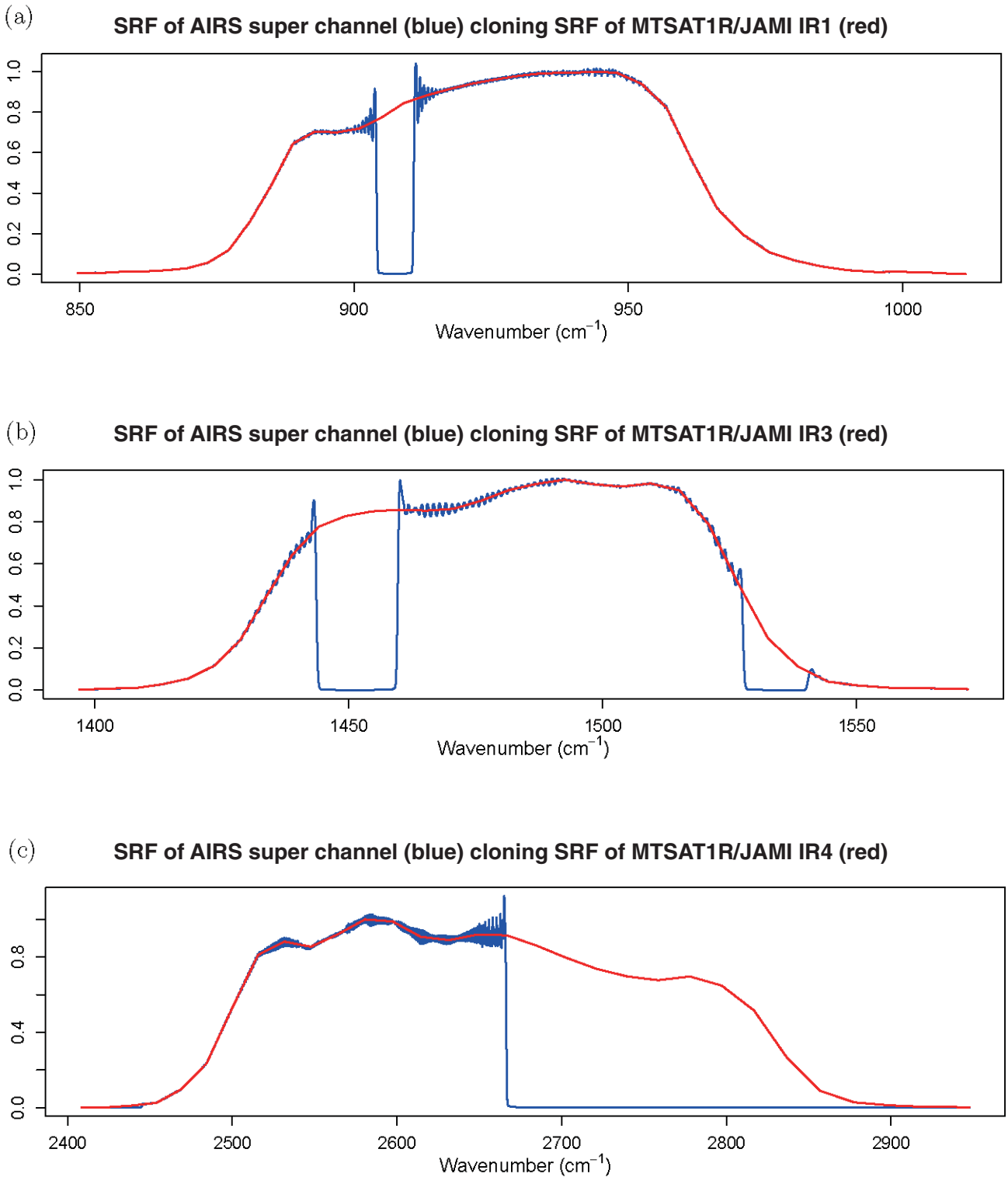

Figure 4: The SRFs of the MTSAT-1R channel IR1 (a), IR3 (b) and IR4 (c) (red) and the AIRS super channels (blue).

3.2 Impacts of missing AIRS channels

As discussed in Section 2.3, the brightness temperature of a super channel varies if some observations of the hyper channels are not available. To estimate this variation, brightness temperature deviations are computed when observing a blackbody. Figure 5 shows the brightness temperature deviations of the AIRS super channels for MTSAT-1R IR2 and IR3 computed by (11) assuming that there is no blacklisted AIRS channel but the observation of one AIRS channel is missing. The vertical axis shows the temperature of the blackbody, and the horizontal axis shows the central wavenumber of the missing AIRS channel.

The central wavenumber of the MTSAT-1R IR2 is 833 cm^{-1} and that of IR3 is 1485 cm^{-1}, respectively. Around the central wavenumbers, the brightness temperature deviation is small, since the AIRS channel radiance there is almost equivalent to the radiance of the super channel, and the lack of the AIRS channel does not change the super channel radiance a lot. Large deviations are recognized where the wavenumber of the missing channel departs from the MTSAT-1R central wavenumber, and the super channel weight of the missing channel is large. However, the largest deviations are small and are about 0.02 K for IR2 and 0.06 K for IR3. Since the accuracy specification of MTSAT-1R brightness temperature observation is 0.21 K, these results indicate that these super channels are applicable if there are a few missing AIRS channels.

3.3 Simulated data comparison

Table 1 shows the simulated brightness

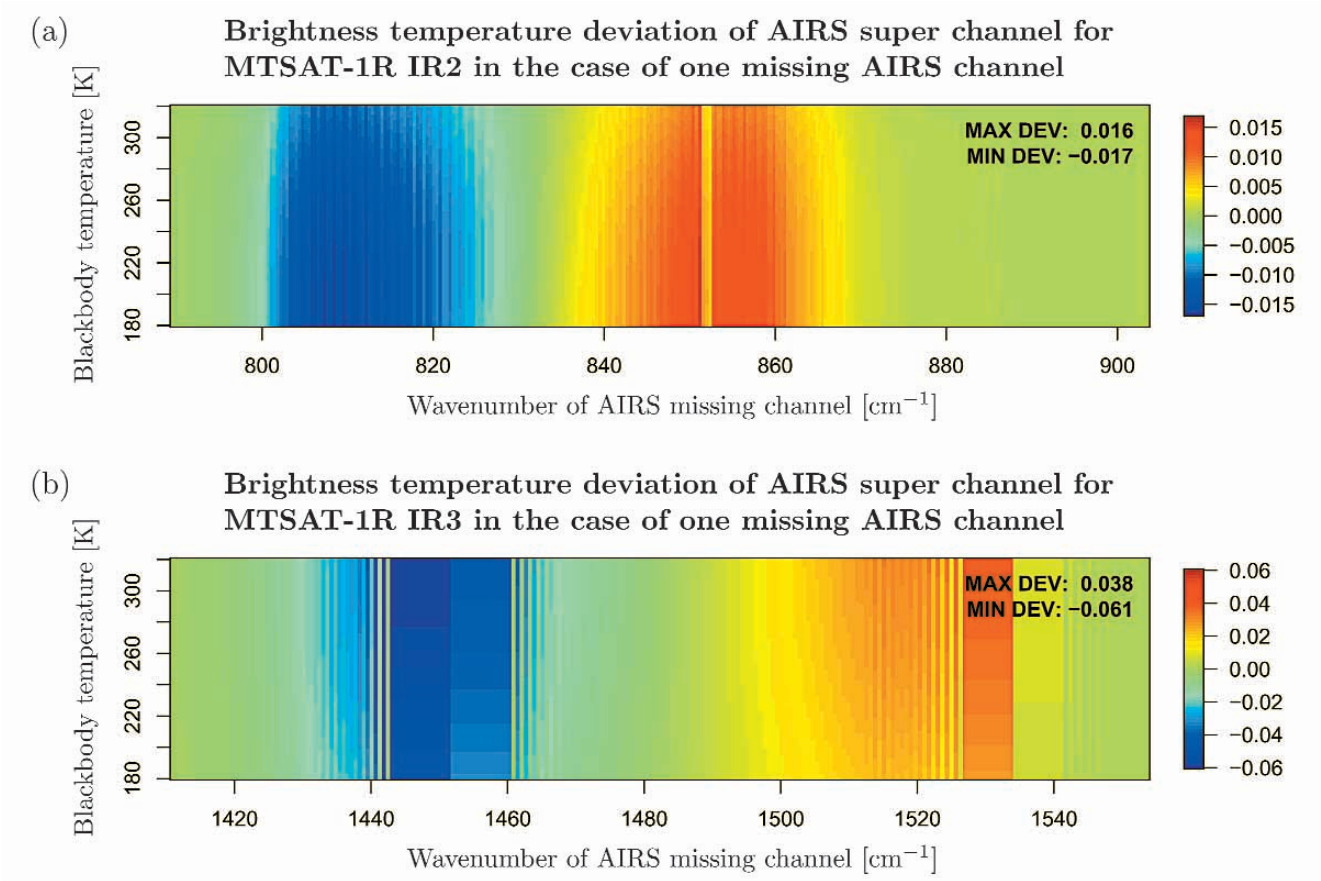

Figure 5: Brightness temperature deviations of the AIRS super channels for MTSAT-1R IR2 (a) and IR3 (b) estimated by Eq. (15) assuming observing a blackbody, no blacklisted channels in AIRS and only one AIRS channel missing. Note that there are the AIRS spectral gaps from 1443 to 1460 cm^{-1} and form 1527 to 1541 cm^{-1}.

temperatures and radiances of the MTSAT-1R infrared channels and the corresponding AIRS super channels as shown in Figures 2 and 4. The simulation uses the line-by-line radiative transfer model LBLRTM (Clough et al., 1995) developed by the Atmospheric and Environmental Research (AER) Inc. with the HITRAN2000 spectroscopic parameters including AER updates (Rothman et al., 2003) and the U.S. standard atmospheric profile. From these comparisons, brightness temperature and radiance differences between the MTSAT-1R infrared channels and the AIRS super channels are estimated, as associated with their spectral response differences assuming that all AIRS channels available and with no calibration and observation errors in the two sensors.

Since the SRF difference between MTSAT-1R IR2 and its AIRS super channel is small as shown in Figure 2, the simulated radiances and brightness temperatures are fairly equal between the two channels. This indicates that the proposed method successfully generates a super channel whose SRF is equivalent to the SRF of the broadband channel.

Since there are AIRS spectral gaps over the observing bands of MTSAT-1R IR1, IR3 and IR4 as shown in Figure 4, radiance differences between the MTSAT-1R channels and the AIRS super channels are larger than the difference recognized in the IR2 comparison. Among the MTSAT-1R three channels, the radiance difference of IR1 is the smallest, since the AIRS spectral gap over the IR1 band is the smallest. As the spectral gaps increases, the radiance differences become larger, and that of IR4 is about 26% and is the largest difference. Therefore, the spectral gaps need to be compensated for when comparing the radiances of AIRS and MTSAT-1R IR1, IR3 and IR4.

When comparing the brightness temperature, the differences between IR1 and IR4 are small and less than the accuracy specification of 0.21 K. Since these channels are located in the infrared window regions where the brightness temperature variation is small, the brightness temperature difference associated with the SRF differences between the red and blue lines, as shown in Figure 4 (a) and (c), is small. Therefore, the brightness temperature comparison of MTSAT-1R IR1 and IR4 with AIRS might be useful without compensating for the SRF differences. The temperature difference for IR3 is 0.3 K and larger than the other channels. This indicates that the SRF difference over the water vapor absorption region may cause larger residual in the brightness temperature comparison as well as the radiance comparison, and the presence of the residual should be taken into account when using the result.

Table 1: Simulated brightness temperatures and radiances of the MTSAT-1R infrared channels and the AIRS super channels. Up-welling radiances from top of atmosphere are simulated the U.S. standard atmosphere by the line-by-line radiative transfer model LBLRTM with the HITRAN2000 line parameters including the AER updates.

MTSAT-1R IR channel		IR1	IR2	IR3	IR4
TB (K)	MTSAT-1R	290.48	289.23	238.26	290.99
	AIRS virtual Ch.	290.53	289.23	237.95	290.92
	Difference	0.05	0.00	0.31	0.07
Radiance ($mW/m^2/sr/cm^{-1}$)	MTSAT-1R	97.23	110.91	5.06	0.477
	AIRS virtual Ch.	97.04	110.92	4.93	0.599
	Difference (%)	0.2	0.01	2.6	25.6

3.4 Real data comparison

Using the AIRS super channels obtained in Section 3.1, intercalibration between MTSAT-1R and AIRS by using real observed data is examined. For the comparison, AIRS level 1B data are downloaded from the Website of NASA, Goddard Earth Sciences Data and Information Services Center (GES DISC). Since no prior information is obtained regarding the accuracy of the AIRS channels, the super channels are generated by using all AIRS channels. The collocation conditions between MTSAT-1R and AIRS data are

Time check : Difference of observing times is within 15 minutes

Position check : Difference of footprint centers is within 5 km

Satellite zenith angle check : Difference of secant satellite zenith angles is within 5%

Uniformity check : IR1 brightness temperature differences between the collocating pixel and its surrounding 5-by-5 pixels are within 3 K

Figure 6 shows brightness temperatures observed by MTSAT-1R IR2 (left), those by the corresponding AIRS super channel (center), and their differences (right). The observation time of the MTSAT-1R data is around 04:40 UTC on November 2, 2006. No uniformity check is applied in the comparison. The observations of 69 out of 333 AIRS channels within the IR2 observing band are missing. Even though such a large number of channels are missing, there is a good correlation in the temperature patterns of the left and middle charts. The chart on the right shows that the MTSAT-1R temperatures are slightly higher than the AIRS ones over the cloud-free regions where the temperatures are high. Over the cloudy regions where the temperatures are low, there are large variations in the temperature

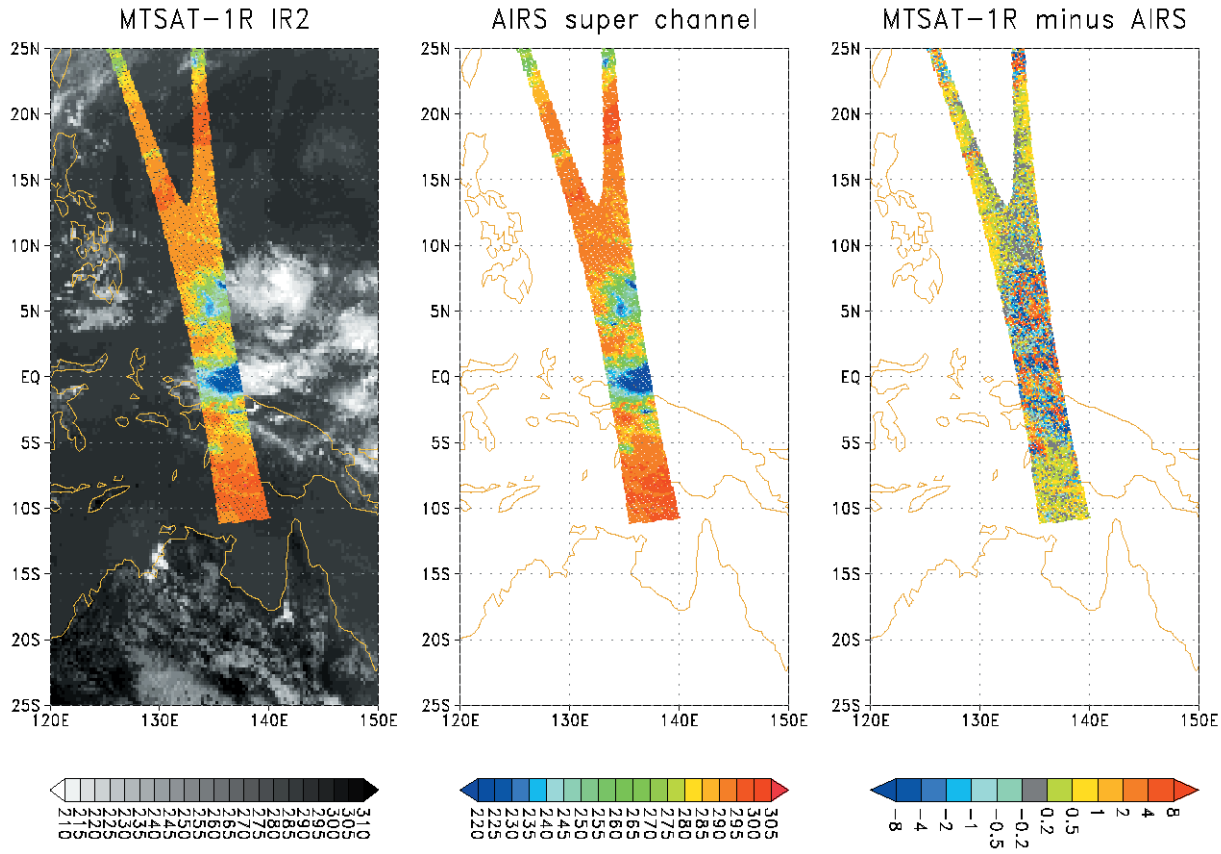

Figure 6: Brightness temperatures observed by the MTSAT-1R channel IR2 (left) and the AIRS super channel (middle) around 04:40 UTC on November 2, 2006. The right chart shows differences between the left and middle charts. The colored points show collected data without applying the uniformity check.

differences on the right chart, and the variations make difficult to recognize any systematical bias.

Figure 7 shows the scatter plot comparison of the brightness temperatures shown in Figure 6, but the uniformity check is applied. The chart on the right is the same as the chart on the left, but the comparison of temperatures higher than 285 K is shown on a magnified scale. The two charts show that the MTSAT-1R IR2 brightness temperatures contain positive biases against the AIRS ones over the whole temperature range. This result corresponds well to the comparison between MTSAT-1R IR2 and the AVHRR channel 5 aboard NOAA-18, shown in Figure 8.

Figure 9 (a) and (b) show the same comparisons as Figure 7 (left) and Figure 8 (left), but for MTSAT-1R IR1. The observations of 122 out of 462 AIRS channels within the IR1 band are missing. Brightness temperature correlation between the MTSAT-1R channels and the AIRS super channels in Figure 9 (a) is high notwithstanding the SRF difference shown in Figure 4 (a). In general, the IR1 temperatures are slightly lower than the AIRS temperatures over a high temperature range, and higher over a low temperature range. The same features are recognized in the comparison between IR1 and the AVHRR channel 4 shown in Figure 9 (b).

Figure 10 shows the same comparison as Figure 9, but for MTSAT-1R IR4. Since the channel IR4 is affected by solar radiance, nighttime data observed around 16:40 UTC are compared. The observations of 14 out of 291 AIRS channels within the IR4 band are missing. As seen in figure (a), there are not enough data obtained over low brightness temperature range in the IR4-AIRS comparison. Over a high temperature range, the average of the IR4 temperatures is slightly lower than that of the AIRS temperatures. This trend is similarly seen in the comparison of IR4 and the AVHRR channel 3B.

Figure 11 shows a comparison of the MTSAT-1R channel IR3 and the AIRS super channel. Since there is no AVHRR channel corresponding to IR3, the

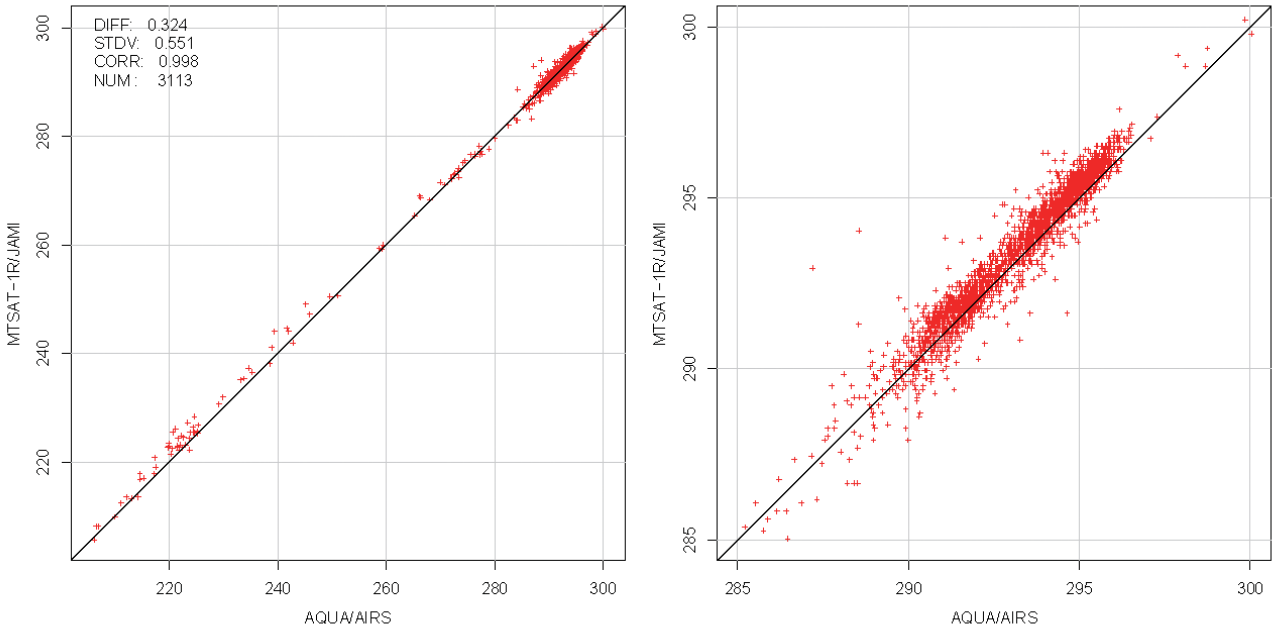

Figure 7: Brightness temperature comparison between the MTSAT-1R channel IR2 and the AIRS super channel. The data shown in Figure 6 are compared after applying the uniformity check. The chart on the right is an enlarged version of the chart on the left over a temperature range higher than 285 K.

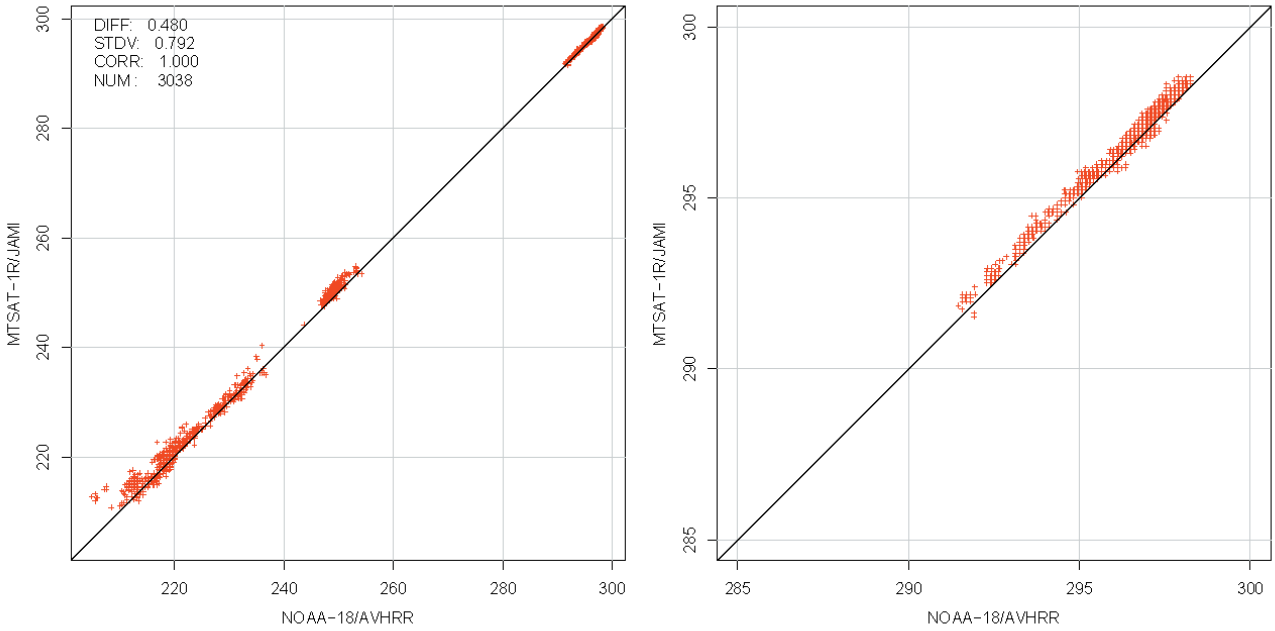

Figure 8: Brightness temperature comparison between the MTSAT-1R channel IR2 and NOAA-18/AVHRR channel 5. The chart on the right is an enlarged version of the chart on the left over a temperature range higher than 285 K. One-month MTSAT-1R IR2 images observed around 04:40 UTC in November 2006 are used for the comparison.

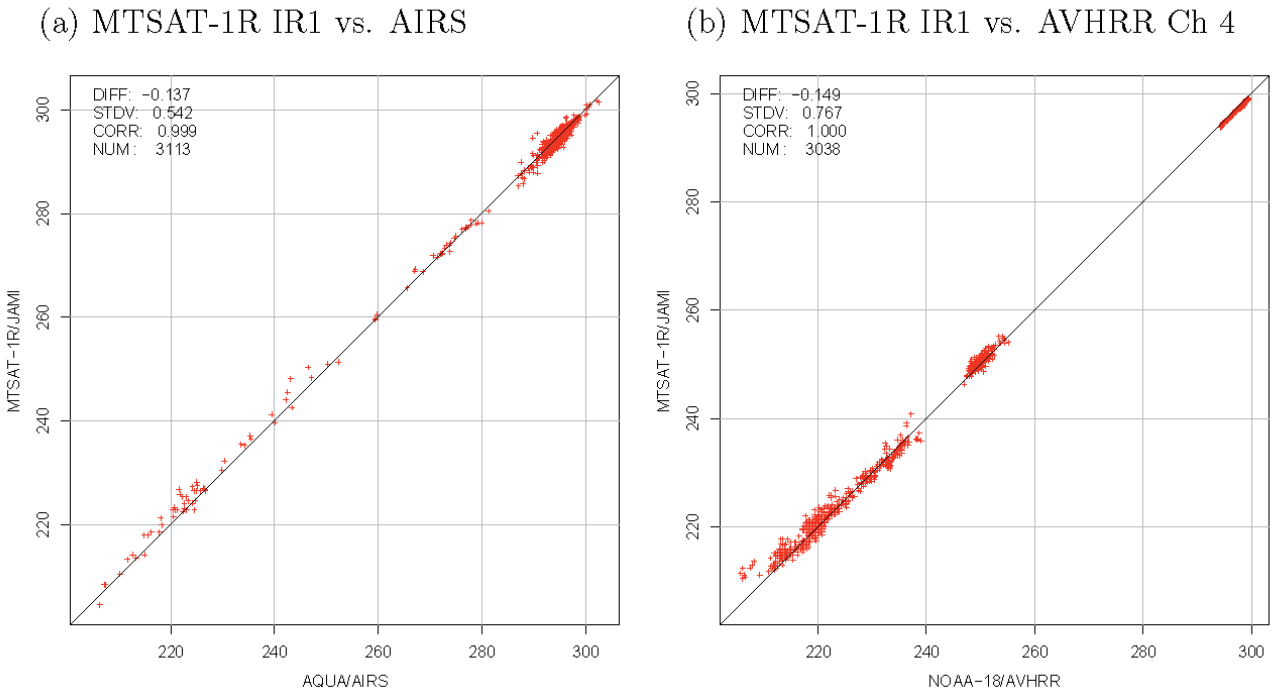

Figure 9: The figure (a) shows brightness temperature comparison between the MTSAT-1R channel IR1 and the AIRS super channel regarding the data observed around 04:40 UTC on November 2, 2006. The figure (b) shows the comparison between IR1 and the NOAA-18/AVHRR channel 4 over one month data observed around 04:40 UTC in November 2006.

comparison between IR3 and AVHRR is not presented. The observations of 26 out of 293 AIRS channels within the IR3 band are missing. The AIRS brightness temperatures correlate well to the IR3 ones.

4 Discussion

Comparisons between the MTSAT-1R infrared channels and the AIRS super channels show that their brightness temperatures are well correlated. Some residuals are also recognized. However, the trend of the residuals is the same as that recognized in the comparison of the MTSAT-1R and NOAA-18/AVHRR infrared channels. The similar residuals recognized in the comparisons of both MTSAT-AIRS and MTSAT-AVHRR might indicate some error involved in the MTSAT-1R infrared calibration. Therefore, the results might indicate the intercalibration using the AIRS super channel is reliable and applicable.

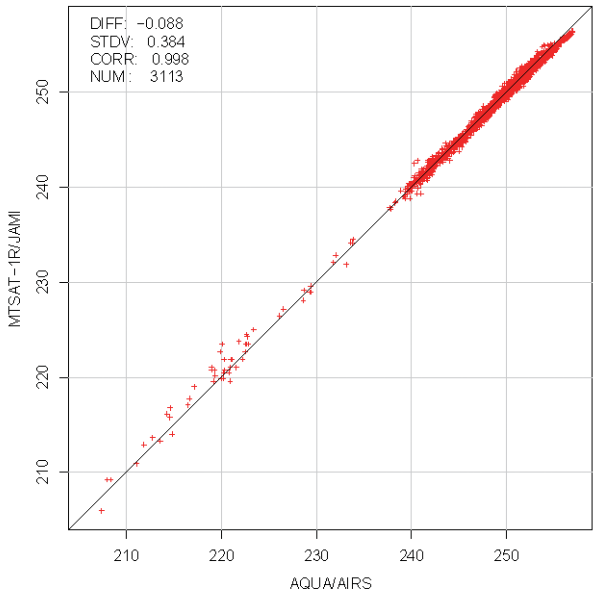

Figure 11: Brightness temperature comparison between the MTSAT-1R channel IR3 and the AIRS super channel. An IR3 image observed around 04:40 UTC on November 2, 2006 is compared with AIRS.

(a) MTSAT-1R IR4 vs. AIRS

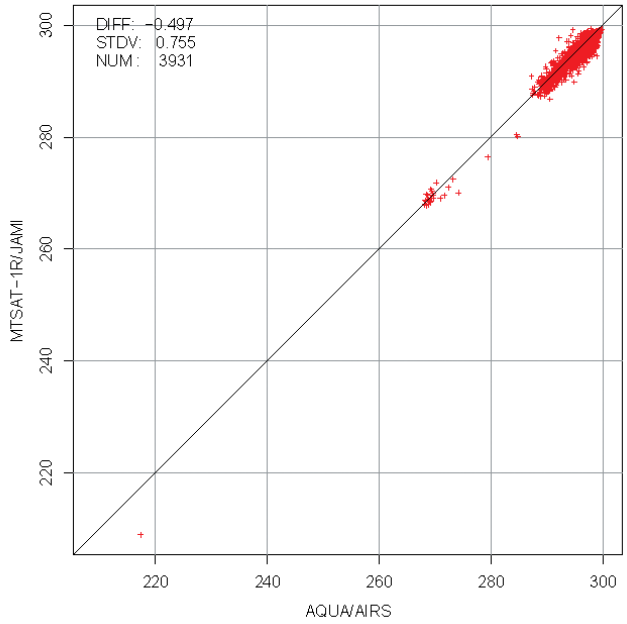

(b) MTSAT-1R IR4 vs. AVHRR Ch 3B

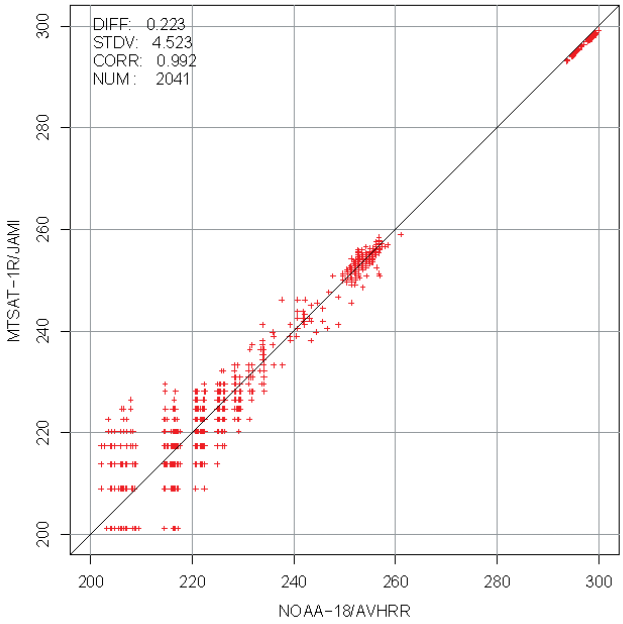

Figure 10: The figure (a) shows brightness temperature comparison between the MTSAT-1R channel IR4 and the AIRS super channel. An IR4 image observed around 17:40 UTC on November 6, 2006 is compared with AIRS. The figure (b) shows the comparison between IR4 and the NOAA-18/AVHRR channel 3B. One-month IR4 images observed around 17:40 UTC in November 2006 are compared with AVHRR data.

However, it should be noted that the results obtained from the comparison of MTSAT-1R and AIRS do not represent exactly the MTSAT-1R calibration error. Spectral response differences between the two sensors remain. There are spectral gaps in the AIRS observing band. There are a lot of AIRS channels whose observations are missing. The number of missing channels is much larger than the number evaluated in the Section 3.2. These factors cause a change in the SRF of the AIRS super channel, and as the result, the brightness temperature transition is not negligible. Before applying the intercalibration using the AIRS super channel, the transition should be evaluated and its amount should be estimated. Using IASI instead of AIRS is another option, since there are no spectral gaps over the infrared band from 645 cm^{-1} to 2760 cm^{-1}. However, the missing observations of the IASI channels should be still evaluated.

5 Summary

A new intercalibration technique using a high spectral resolution sounder (hyper sounder) is presented. This technique generates a super channel cloning a broadband one from the hyper sounder channels (hyper channels) by minimizing the spectral response difference between the broadband and super channel.

The techniques are evaluated by comparing the simulated radiance of the MTSAT-1R imager and AIRS. The results show that the brightness temperature and radiance of the AIRS super channel for the MTSAT-1R channel IR2 are nearly equivalent to those of IR2. That indicates that the techniques are applicable to conditions in which the hyper channels cover the whole spectral band of the broadband channel if there are no missing hyper channel observations and no calibration and observation error is involved in the hyper channels.

The comparison of observed data between MTSAT-1R and AIRS is also examined. Brightness temperature residuals between MTSAT-1R IR2 and AIRS show a similar trend to those between IR2 and the NOAA-18/AVHRR channel 5, even though there are a large number of AIRS channels missing within the IR2 spectral band. A similarity is also recognized in the comparison of MTSAT-1R IR1 and IR4 with the AIRS super channels, even though there are spectral differences between the MTSAT-1R channels and the AIRS super ones in addition to many missing AIRS channels. This similarity might indicate that the intercalibration using the AIRS super channel is reliable and applicable.

However, it should be noted that the results obtained from the comparison of MTSAT-1R and AIRS does not represent exactly MTSAT-1R calibration error owing to the existence of the AIRS spectral gaps and missing observations in the AIRS channels, and there is no compensation for the calibration and observation error of the AIRS channels. For a more accurate comparison, the evaluation and compensation of these factors degrading intercalibration accuracy should be studied further.

References

Clough, S. A., and M. J. Iacono, 1995: Line-by-line calculations of atmospheric fluxes and cooling rates II: Application to carbon dioxide, ozone, methane, nitrous oxide, and the halocarbons. J. Geophys. Res., 100. 16519-16535.

Gunshor, M. M., T. J. Schmit, W. P. Menzel, and D. C. Tobin, 2006: Intercalibration of the newest geostationary imagers via high spectral resolution AIRS data. Conference on Satellite Meteorology and Oceanography, 14th, Atlanta, GA, January29-February 2, 2006 (preprints). Boston, MA, American Meteorological Society, 2006, Paper P6.13.

Rothman et al., 2003: The HITRAN molecular spectroscopic database: edition of 2000 including updates through 2001, Journal of Quantitative Spectroscopy and Radiative Transfer. vol. 82, 5-44.

Tahara, Yoshihiko, Nozomu Ohkawara, and Arata Okuyama, 2004: Intercalibration of the Infrared Channels between GMS-5 and GOES-9. Meteorological Satellite Center Technical Note, No. 44, 1-18 (written in Japanese).

Tobin, D. C., H. E. Revercomb, C. C. Moeller, and T. Pagano, 2006: Use of Atmospheric Infrared Sounder high-spectral resolution spectra to assess the calibration of Moderate re solution Imaging Spectroradiometer on EOS Aqua, J. Geophys. Res., 111, D09S05, doi:10.1029/2005JD006 095.

Weinreb, M. P., Fleming, H. E., McMillin, L. M. and Neuendorffer, A. C., 1981: Transmittances for the TIROS Operational Vertical Sounder. NOAA Tech. Rep. NESS 85.

Webpages

Atmospheric and Environmental Research (AER), Inc.: AERのs Radiative Transfer Working Group. http://rtweb.aer.com/main.html

Meteorological Satellite Center (MSC): Monitoring of MTSAT-1R Navigation and Calibration. http://mscweb.kishou.go.jp/monitoring/mtsat_monit.htm

National Aeronautics and Space Administration (NASA): Goddard Earth Sciences (GES) Data and Information Services Center (DISC). http://daac.gsfc.nasa.gov/

National Aeronautics and Space Administration (NASA), Jet Propulsion Laboratory (JPL): Atmospheric Infrared Sounder (AIRS). http://www-airs.jpl.nasa.gov/

University of Maryland, Baltimore County (UMBC), Atmospheric Spectroscopy Laboratory (ASL): Atmospheric Infrared Sounder (AIRS). http://asl.umbc.edu/pub/airs/airs.html

---

高スペクトル分解能サウンダを利用したインターキャリブレーションに関する新しい手法の提案

太原　芳彦*

要　旨

高スペクトル分解能サウンダ（ハイパーサウンダ）を利用した、広い観測スペクトル帯域を持つセンサとのインターキャリブレーションについて、広帯域チャネルの応答関数とのズレを最小にする疑似チャネルを作成して行う新しい手法を考案した。 そして、この手法に基づき、アメリカ航空宇宙局(NASA)のハイパーサウンダAIRSと、広帯域チャネルを持つMTSAT-1Rイメージャとの比較を試みた。放射シミュレーションを利用して、AIRS観測に誤差や欠測が無い理想的な場合を想定したMTSAT-1R IR2チャネルとそのAIRS疑似チャネルの比較結果は、AIRSの観測帯域がMTSAT-1R IR2の観測帯域全体を包括し、AIRS疑似チャネルの応答関数がIR2のそれと適合するため、放射輝度と輝度温度が共に良く一致することが確認された。 実データを利用したMTSAT-1RとAIRSとの比較結果は、AIRSに欠測チャネルが多く含まれる、AIRSにはIR2以外のチャネルの一部帯域に空白がある、AIRS観測の誤差が不明であるにも関わらず、MTSAT-1RとNOAA-18搭載イメージャAVHRRとの比較結果と傾向が良く一致し、本手法の有効性が示された。

* 気象衛星センターデータ処理部 システム管理課